ISSN 1674-1056
http://cpb.iphy.ac.cn
http://iopscience.iop.org/cpb
中国物理 B
Chinese Physics
中国物理
Chinese Physics B

Numerical investigation on coherent mid-infrared supercontinuum generation in chalcogenide PCFs with near-zero flattened all-normal dispersion profiles

Jie Han(韩杰)[1], Sheng-Dong Chang(常圣东)[2], Yan-Jia Lyu(吕彦佳)[1], Yong Liu(刘永)[1]
Citation: Chin. Phys. B . 2019, 28(10): 104204 . **doi:** 10.1088/1674-1056/ab3f25
Journal homepage: http://cpb.iphy.ac.cn; http://iopscience.iop.org/cpb

What follows is a list of articles you may be interested in

The 2-μm to 6-μm mid-infrared supercontinuum generation in cascaded ZBLAN and As_2Se_3 step-index fibers

Jinmei Yao(姚金妹), Bin Zhang(张斌), Ke Yin(殷科), Jing Hou(侯静)
Chin. Phys. B . 2019, 28(8): 084209 . **doi:** 10.1088/1674-1056/28/8/084209

Supercontinuum generation of highly nonlinear fibers pumped by 1.57-μm laser soliton

Song-Tao Fan(樊松涛), Yan-Yan Zhang(张颜艳), Lu-Lu Yan(闫露露), Wen-Ge Guo(郭文阁), Shou-Gang Zhang(张首刚), Hai-Feng Jiang(姜海峰)
Chin. Phys. B . 2019, 28(6): 064204 . **doi:** 10.1088/1674-1056/28/6/064204

Monolithic all-fiber mid-infrared supercontinuum source based on a step-index two-mode As_2S_3 fiber

Jinmei Yao(姚金妹), Bin Zhang(张斌), Jing Hou(侯静)
Chin. Phys. B . 2019, 28(6): 064205 . **doi:** 10.1088/1674-1056/28/6/064205

Mid-infrared supercontinuum generation and its application on all-optical quantization with different input pulses

Yan Li(李妍), Xinzhu Sang(桑新柱)
Chin. Phys. B . 2019, 28(5): 054206 . **doi:** 10.1088/1674-1056/28/5/054206

Supercontinuum manipulation based on the influence of chirp on soliton spectral tunneling

Saili Zhao(赵赛丽), Huan Yang(杨华), Yilin Zhao(赵奕霖), Yuzhe Xiao(肖宇哲)
Chin. Phys. B . 2018, 27(11): 114219 . **doi:** 10.1088/1674-1056/27/11/114219

Numerical investigation on coherent mid-infrared supercontinuum generation in chalcogenide PCFs with near-zero flattened all-normal dispersion profiles*

Jie Han(韩杰)[1,†], Sheng-Dong Chang(常圣东)[2], Yan-Jia Lyu(吕彦佳)[1], and Yong Liu(刘永)[1]

[1] State Key Laboratory of Electronic Thin Film and Integrated Devices, School of Optoelectronic Science and Engineering, University of Electronic Science and Technology of China, Chengdu 610054, China

[2] School of Environment, 3480 University Street, McGill University, Montréal H3A 0E9, Canada

(Received 11 April 2019; revised manuscript received 23 July 2019; published online 17 September 2019)

We design a novel all-normal flat near-zero dispersion chalcogenide photonic crystal fiber (PCF) for generating mid-infrared (MIR) supercontinuum (SC). The proposed PCF with a core made of As_2Se_3 glass and uniform air holes in the cladding is selectively filled with As_2S_5 glass. By carefully engineering the PCF with an all-normal flat near-zero dispersion profile, the anomalous-dispersion soliton effect is reduced, thus enabling broadband highly coherent SC to be generated. We also investigate the influence of the pulse parameters on the SC generation. Broadband SC covering 1.4 μm–10 μm with perfect coherence is achieved by pumping the proposed 3-cm-long PCF with 3-μm 100-fs pulses. The results provide a potential all-fiber realization of the broadband coherent MIR-SC.

Keywords: supercontinuum generation, photonic crystal fiber, nonlinear optics

PACS: 42.81.–i, 42.65.–k, 42.65.Sf **DOI:** 10.1088/1674-1056/ab3f25

1. Introduction

Coherent light sources in mid-infrared (MIR) region are of great significance for scientific and engineering applications in many domains such as medical surgery,[1] remote sensing,[2] and military countermeasure,[3] since a large number of molecules display a strong vibration absorption capability in this region. The supercontinuum (SC) generation is a process that generates a broad spectrum, promoting the applications in the relevant fields above. Silica-based glass fibers have proved to be excellent nonlinear medium for SC generation. However, the strong material absorption of silica fibers in the MIR region ($>$ 2.5 μm) limits their applications at longer wavelengths. Compared with silica fibers, chalcogenide glass fibers benefit from their wide transmission window up to 20 μm,[4] thus making them a superior candidate for MIR-SC generation. To date, MIR-SC generation spanning from 2 μm to 16 μm has been successfully demonstrated by using a chalcogenide fiber as a nonlinear medium.[5] Appropriate pump wavelength also plays a crucial role in wide SC generation. It needs to be in the anomalous dispersion regime and near the zero dispersion wavelength of the said fiber.[5] The spectral broadening is mainly dominated by soliton dynamics, especially soliton fission, and subsequent soliton self-frequency shift. However, soliton dynamics is sensitive to the input noise,[6] which causes the spectral coherence to degrade. In view of the perspective of practical applications, the SCs with high coherence possesses great applications in optical coherence tomography[7] and frequency metrology.[8]

To generate coherent SCs, fibers with all-normal dispersion profiles are now used. For SCs in these fibers, spectrum broadening is mainly dominated by self-phase modulation (SPM) and optical wave breaking (OWB), which suppress soliton-related process, especially soliton fission. The generated SC possesses perfect coherence in the entire spectrum. In the following experimental work the all-normal dispersion fibers are adopted for better SC coherence.[9–13] Al-Kadry *et al.* generated a 0.96-μm–2.5-μm coherent SC by using 150-pJ pulses to pump all-normal dispersion chalcogenide microwires.[9] A coherent SC covering 2.2 μm–3.3 μm was demonstrated by using all-normal dispersion $AsSe_2$–As_2S_5 microstructured fiber pumped at 2.7 μm.[10] Nagasaka *et al.* used a double-cladding chalcogenide fiber, which has As_2Se_3 core and $AsSe_2$ inner cladding and As_2S_5 outer cladding, pumped with 1.3-MW pulses at 10 μm to generate 2-μm–14-μm coherent SC.[11] Optical parametric amplifier (OPA) was adopted because the considered pump pulse is hard to obtain just by fiber laser. However, OPA suffers huge system and high expanse, which is disadvantageous to the practical applications. Jiao *et al.* generated a coherent SC covering 2 μm–14 μm by pumping a double-cladding tellurium fiber with femtosecond laser at 5 μm.[12] The choice of the double-cladding fiber leads to the high peak power (estimated at around several megawatts) of the pump pulses. In addition, OPA was also used to provide pump pulses. Zhang *et al.* generated a coherent SC covering 1.7 μm–12.7 μm by pumping a

*Project supported by the National Natural Science Foundation of China (Grant Nos. 61421002 and 61435003).

†Corresponding author. E-mail: jiehan@std.uestc.edu.cn

© 2019 Chinese Physical Society and IOP Publishing Ltd

chalcogenide tapered fiber at 5.5 μm.[13] The adopted dispersion curve is inverted-V-shaped. The long wavelength components experience large group velocity dispersion, which also means that high pump power leads to a large red frequency shift.

There are also several numerical simulations on SCs in all-normal dispersion medium. Karim *et al.* numerically demonstrated a 2-μm–5.5-μm SC by pumping a $Ge_{11.5}As_{24}Se_{64.5}$ PCF with 5-kW pulses at 3.1 μm.[14] Then Singh Saini *et al.* simulated coherent SC covering 1.2 μm–7.2 μm by pumping a chalcogenide rib waveguide at 2.8 μm.[15] Nagasaka *et al.* numerically generated a coherent SC covering 3.3 μm–10.4 μm by pumping a chalcogenide double-clad fiber with 300-fs pulses at 6 μm.[16] The considered pump pulses are still based on OPA. Diouf *et al.* numerically generated a coherent SC covering 2.9 μm–4.575 μm by pumping an $As_{38.8}Se_{61.2}$ PCF with 50-fs pulses at 3.7 μm.[17] The adopted dispersion curve is also inverted-V-shaped, which is disadvantageous to increasing red frequency shift due to the large dispersion of long wavelength components.[18] Cherif *et al.* generated a 2 μm–8 μm coherent SC by pumping an As_2Se_3-based PCF with pulses at 5 μm.[19] The adopted dispersion curve is inverted-V-shaped, and the pump pulse is hard to obtain by fiber laser.

Appropriate all-normal dispersion profile is significant for the broadband coherent SC generation. Compared with the inverted-V-shaped dispersion curve, an inverted-L-shaped dispersion curve is very beneficial to increasing red frequency shift of the SC.[18] To obtain such inverted-V-shaped dispersion characteristics, fibers with high design flexibility are more attractive. Having high design flexibility and being able to achieve the desired dispersion characteristics, the photonic crystal fibers (PCFs) enjoy the dispersion curve that is changeable by varying the geometric parameters, and the nonlinearity of PCF can also increase due to the enhanced confinement of the optical field. All the above merits of PCFs are favorable for generating broadband SC in the MIR region.

In this paper, we design a novel 3-cm-long As_2Se_3–As_2S_5 PCF with near-zero flattened all-normal dispersion profiles. With the above all-normal dispersion PCF, it is possible to generate SC up to 10 μm with perfect coherence when pumped with pulses at 3 μm, and the resulting SC is able to cover two atmospheric windows of 3 μm–5 μm and 8 μm–10 μm wavelengths. Our simulations provide a potential all-fiber scheme to obtain highly coherent MIR-SC.

2. Numerical model

Pulse propagation in the fiber can be modeled by generalized nonlinear Schrödinger equation (GNLSE). Based on the derivation of GNLSE in Ref. [20], we solved this equation in the frequency domain:

$$\frac{\partial \tilde{A}'}{\partial z} = \mathrm{i}\bar{\gamma}(\omega)\exp\left(-\hat{L}(\omega)z\right)F \times\left\{\bar{A}(z,T)\int_{-\infty}^{+\infty}R(T')\left|\bar{A}(z,T-T')\right|^2\mathrm{d}T'\right\}, \quad (1)$$

where $\hat{L}(\omega)$ is the linear operation, which models linear propagation effects and is defined as

$$\hat{L}(\omega)=\mathrm{i}\left(\beta(\omega)-\beta(\omega_0)-\beta_1(\omega_0)[\omega-\omega_0]\right)-\frac{\alpha(\omega)}{2}, \quad (2)$$

where $\alpha(\omega)$ denotes the frequency-dependent linear loss in the fiber, $\beta(\omega)$ the propagation constant, ω the angular frequency, ω_0 the central angular frequency, and $\bar{\gamma}(\omega)$ the frequency-dependent nonlinear coefficient, which is defined as

$$\bar{\gamma}(\omega)=\frac{n_2 n_0 \omega}{c n_{\mathrm{eff}}(\omega)A_{\mathrm{eff}}^{1/4}(\omega)}, \quad (3)$$

where n_2 is the nonlinear refractive index, and $n_{\mathrm{eff}}(\omega)$ is the frequency-dependent refractive index. It should be noted that this definition of nonlinear coefficient is different from the conventional definition of nonlinear coefficient that is defined as

$$\gamma(\omega)=\frac{n_2\omega}{cA_{\mathrm{eff}}(\omega)}. \quad (4)$$

$\bar{A}(z,T)$ is defined as

$$\bar{A}(z,T)=F^{-1}\left\{\frac{\tilde{A}(z,\omega)}{A_{\mathrm{eff}}^{1/4}(\omega)}\right\}, \quad (5)$$

where $A_{\mathrm{eff}}(\omega)$ denotes the frequency-dependent effective area, which is given by

$$A_{\mathrm{eff}}(\omega)=\frac{\left(\int\int_{-\infty}^{+\infty}|F(x,y,\omega)|^2\mathrm{d}x\mathrm{d}y\right)^2}{\int\int_{-\infty}^{+\infty}|F(x,y,\omega)|^4\mathrm{d}x\mathrm{d}y}, \quad (6)$$

where $F(x,y,\omega)$ is the transverse mode distribution in the fiber and $R(t)$ is the nonlinear response function which can be obtained from

$$R(t)=(1-f_{\mathrm{R}})\delta(t)+f_{\mathrm{R}}h_{\mathrm{R}}(t), \quad (7)$$

where f_{R} denotes the Raman contribution to the total nonlinear response and $h_{\mathrm{R}}(t)$ represents the delayed Raman response and is expressed as a damped oscillation function, which is given by

$$h_{\mathrm{R}}(t)=\frac{\tau_1^2+\tau_2^2}{\tau_1\tau_2^2}\exp\left(-\frac{t}{\tau_2}\right)\sin\left(\frac{t}{\tau_1}\right). \quad (8)$$

Using

$$\tilde{A}'(z,\omega)=\tilde{A}(z,\omega)\exp\left(-\hat{L}(\omega)z\right) \quad (9)$$

to change into interaction picture, the stiff dispersive part of the equation can be removed.[21] This version of GNLSE can be solved by standard Runge–Kutta method.

Shot noise of the input pulses is added based on the one photon per mode (OPPM) model,[22] which is defined as

$$\tilde{A}_{\text{noise}}(\nu) = \sqrt{T_{\max} h\nu}\exp[\mathrm{i}\varphi(\nu)], \tag{10}$$

where $T_{\max}$ is the time window of the simulation, h the Planck constant, ν the frequency, and $\varphi(\nu)$ the random phase described by the white noise which is uniformly distributed in the interval of $[0, 2\pi]$. The OPPM noise model is added in the frequency domain, then the field with random noise is transformed into the time domain to denote the input pulse.

The coherence can be described by the modulus of the complex degree of first-order coherence,[6] which is defined as

$$\left|g_{12}^{(1)}(\lambda, t_1 - t_2)\right| = \left|\frac{\langle E_1^*(\lambda, t_1) E_2(\lambda, t_2)\rangle}{\sqrt{\left\langle |E_1(\lambda, t_1)|^2\right\rangle \left\langle |E_2(\lambda, t_2)|^2\right\rangle}}\right|, \tag{11}$$

where the angular brackets denote an ensemble average of a great number of independently generated pairs of SC spectra $[E_1(\lambda, t), E_2(\lambda, t)]$, and t is the time measured on the scale of the temporal resolution of the spectrometer used to resolve these spectra. The degree of coherence $|g_{12}^{(1)}|$ lies in the interval [0,1], with a value of 1 denoting perfect coherence.

3. Design of all-normal dispersion chalcogenide PCF

The conventional hexagon PCF structure is adopted to obtain all-normal dispersion properties. The cross-section of the proposed chalcogenide PCF is shown in Fig. 1, where d is the air hole diameter and Λ is the pitch between two air holes. The PCF has a core made of As_2Se_3 surrounded by five rings of circular air holes where the innermost ring is filled with As_2S_5 glass. The As_2Se_3 glass and the As_2S_5 glass each have a high transmissivity in the region of 1 μm–17 μm and 1 μm–15 μm,[11] respectively. All these holes have identical diameters. Such a microstructured fiber can be fabricated by rod-in-tube technique.[23]

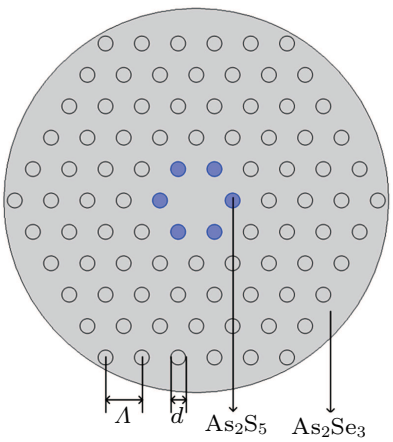


Fig. 1. Cross-section of the proposed As_2Se_3–As_2S_5 PCF.

3.1. Dispersion properties of PCF

The wavelength-dependent refractive index of the chalcogenide glass is calculated from the Sellmeier equation

$$n^2(\lambda) = 1 + \sum_i \frac{A_i \lambda^2}{\lambda^2 - \lambda_i^2}. \tag{12}$$

Here, the coefficients A_i and λ_i of As_2Se_3 and As_2S_5 are cited from Refs. [24] and [23], respectively. The group velocity dispersion (GVD) of the fiber is calculated from

$$D = -\frac{\lambda}{c}\frac{\mathrm{d}^2 n_{\text{eff}}}{\mathrm{d}\lambda^2}, \tag{13}$$

where n_{eff} is the effective refractive index calculated by COMSOL based on the full-vector finite element method.

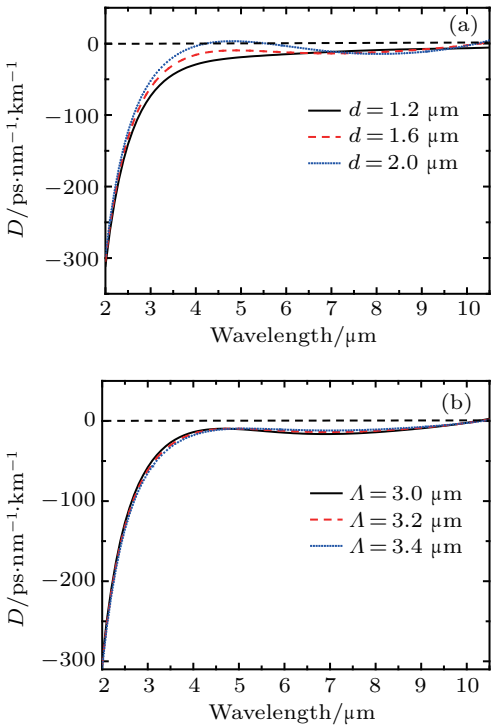


Fig. 2. Plots of D *versus* wavelength (a) for three different d values and (b) for three different Λ values, respectively.

To obtain all-normal dispersion property of the proposed PCF, we optimized the dispersion by changing the structure parameters of the fiber. Dispersion curves of the PCF can be changed by varying the values of air hole diameter d, and the pitch Λ. Figure 2 shows the dispersion curves of the proposed PCF in a wavelength range between 2 μm and 10 μm. The dispersion curves with fixed Λ value at 3.2 μm and varying d value are shown in Fig. 2(a). As can be observed in Fig. 2(a), when the air hole diameter increases, the dispersion curve moves up. When d value is smaller than 2 μm, the whole dispersion curves are below the zero axis. When d value increases to 2 μm, the peak of the dispersion curve enters into the anomalous dispersion region, which is related to soliton dynamics that can cause the SC coherence to degrade. The

dispersion curve with d value at 1.6 μm has the near zero flatted all-normal property in a 4 μm–10 μm region. To investigate the effect of Λ value on the dispersion characteristics, we calculated the dispersion by changing Λ value. The dispersion curves with fixed d value at 1.6 μm and varying Λ value are shown in Fig. 2(b). When Λ value changes, dispersion curves are nearly unchanged. For varying Λ value at 3.0 μm, 3.2 μm, and 3.4 μm, all three dispersion curves are in the normal dispersion region. According to the dispersion curves mentioned above, we chose the chalcogenide PCF with d value at 1.6 μm and Λ value at 3.2 μm as the optimized all-normal dispersion fiber. The corresponding dispersion curve is shown in the red dashed line in Fig. 2(a).

3.2. Effective mode area and nonlinear coefficient of PCF

The effective mode area and the nonlinear coefficient are calculated by Eq. (6) and Eq. (4), respectively, which are shown in Fig. 3. The value of n_2 is 2.3×10^{-17} m^2/W.[1] The black line and the red line indicate the effective mode area and the nonlinear coefficient, respectively. As can be observed in Fig. 3, the efficient mode area increases with wavelength increasing, while the nonlinear coefficient has an opposite trend. The effective area and the nonlinear coefficient at 3 μm are 15 μm^2 and 3.22 W^{-1}·m^{-1}, respectively.

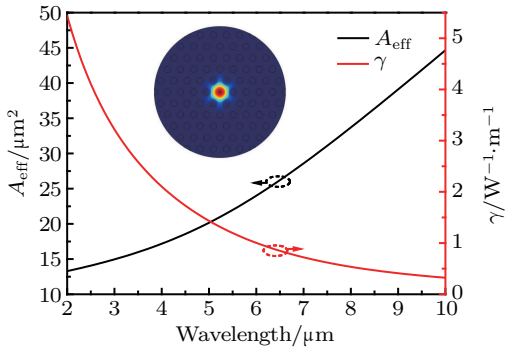


Fig. 3. Calculated effective mode area and nonlinear coefficient *versus* wavelength of proposed all-normal dispersion PCF ($\Lambda = 3.2$ μm, and $d =$ 1.6 μm), with inset showing fundamental mode distribution at 3 μm of proposed PCF.

4. Results and discussion

According to the obtained all-normal dispersion curve, first, we numerically study the chalcogenide PCF pumped with hyperbolic secant pulses at 3 μm, which can be obtained in an Er^{3+}-doped ZBLAN fiber laser.[25] The fundamental mode distribution at 3 μm of the proposed PCF is shown in the inset in Fig. 3, which indicates that the optical field is confined in the PCF core. The GVD at 3 μm has a value of −61.7 ps·nm^{-1}·km^{-1}. For As_2Se_3-based fiber, $f_{\rm R} = 0.148$, $\tau_1 = 23$ fs, and $\tau_2 = 164.5$ fs are considered in the simulation.[26] In order to investigate the effect of pulse parameters (peak power and pulse width) on the obtained SC, we solve the GNLSE by MATLAB with a series of varying pulse parameters.

We first pump 3-cm PCF with 100-fs pulses. The obtained spectra at the output of the PCF pumped with 4 kW–16 kW are shown in Fig. 4. The obtained spectrum width increases with peak power increasing. As the pump peak power increases, the short wavelength edges of the generated SCs decrease little while the long wavelength edges increase obviously. When the peak power reaches 16 kW, the generated SC covers the wavelength region from 1.4 μm to 9.9 μm at a −40-dB level. The long wavelength edge is nearly 10 μm.

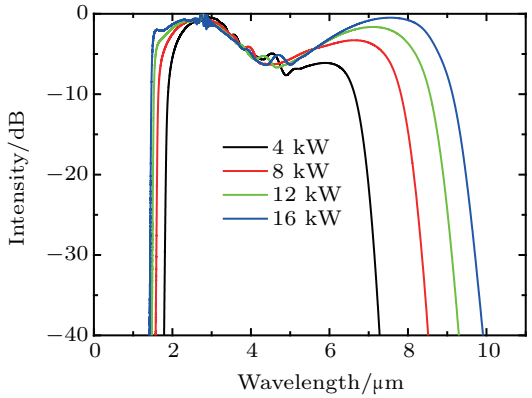


Fig. 4. Simulated output spectra in 3-cm PCF ($\Lambda = 3.2$ μm, $d = 1.6$ μm) when pumped at 3 μm with 4-kW–16-kW pulses (pulse width: 100 fs).

When the peak power increases to 16.8 kW, the output SC rises from 1.4 μm to 10 μm. The corresponding spectral and temporal evolution along the 3-cm chalcogenide PCF are shown in Figs. 5(a) and 5(b), respectively. At the first stage of the SC generation, self-phase modulation is dominated. This causes the spectrum to broaden symmetrically. After several millimeters' propagation, the spectrum broadening is dominated by optical wave breaking. Because the pulse propagates in the normal dispersion region, longer wavelength components travel faster than shorter wavelength components, which causes different wavelengths to overlap in the time domain.[27] This phenomenon results in the generation of new frequencies on both sides of the spectrum. The onset position of OWB can be calculated from

$$L_{\rm wb} = \frac{T_0^2}{\beta_2}\sqrt{\frac{3\beta_2}{2\beta_2 + 2\gamma P_0 T_0^2}}, \tag{14}$$

where T_0 is the pulse width, β_2 is the group velocity dispersion, and P_0 is the peak power of the pulse.[15,27] The calculated onset distance of OWB is 0.5 mm. It means that the OWB occurs at the very short distance, which can be observed from Fig. 5(a). The corresponding spectral and temporal output are depicted in Figs. 5(c) and 5(d), respectively.

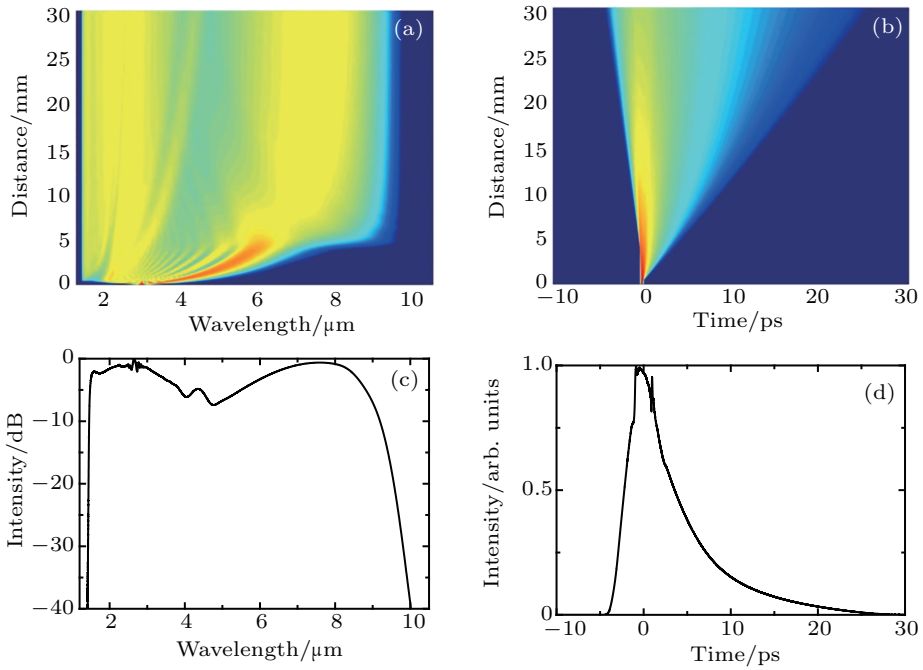


Fig. 5. (a) Simulated spectral and (b) temporal evolutions along the fiber, (c) simulated spectral output, and (d) simulated temporal output, obtained on condition that 3-cm chalcogenide PCF is pumped at 3 μm with 100-fs pulses with 16.8-kW peak power.

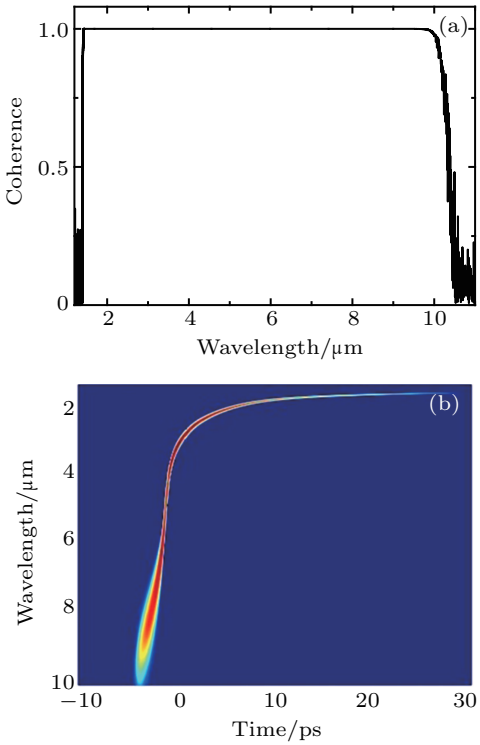


Fig. 6. (a) Simulated modulus of complex degree of first-order coherence and (b) spectrogram of the output SC, with 3-cm chalcogenide PCF pumped at 3 μm by 100-fs pulse with 16.8-kW peak power.

To investigate the coherence characteristics of the generated SC, we conduct 20 independent simulations with random noise described by OPPM model, which generates 190 pairs of SC spectra. The calculated modulus of complex degree of first-order coherence of the output SC is shown in Fig. 6(a). As can be seen from the figure, the degree of coherence has a value of 1 in the entire spectrum, which indicates perfect coherence. The spectrogram can reveal spectral and temporal characteristics of pulses simultaneously. The corresponding spectrogram is depicted in Fig. 6(b). It shows that the obtained SC has no separated components in both time domain and frequency domain, which further confirms the coherent characteristics.

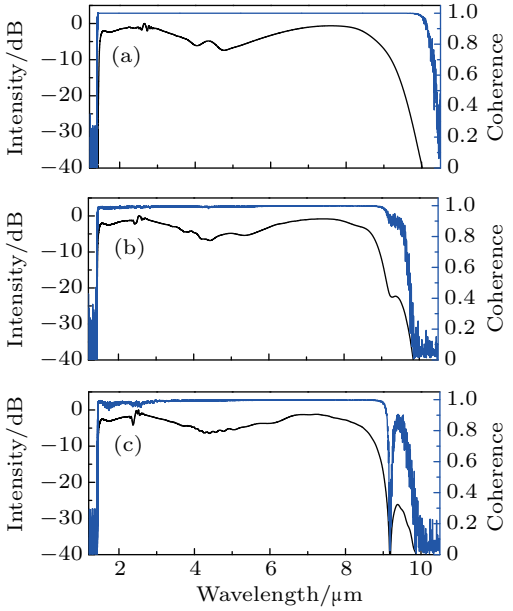


Fig. 7. Simulated spectra and coherence of the generated SCs, with 3-cm chalcogenide PCF pumped at 3 μm by pulses with peak power of 16.8 kW and pulse duration of (a) 100 fs, (b) 200 fs, and (c) 300 fs, respectively.

To investigate the influence of pulse width on the SC, we carry out simulations by changing pulse widths. Figure 7 shows the spectra and coherence of the generated SCs when pumped at 3 μm with 100-fs–300-fs pulses. As pulse width

increases, the spectrum has more oscillation components, and the spectrum width decreases. Compared with longer pulse duration, shorter pulse duration undergoes stronge SPM effect, which causes a wider SC spectrum at the same distance. When pump pulse duration increases, the generated SC is still highly coherent. By using ultra-short pulses, broadband and highly coherent SC can be obtained.

The pump wavelengths of the simulations mentioned above are 3 μm. At this pump wavelength, the dispersion of the PCF is -61.7 ps·nm^{-1}·km^{-1}. A smaller value of dispersion is beneficial to the low pump power. The optimized dispersion curve has near-zero flatted characteristics in a region of 4 μm–10 μm, which provides the wide selection of pump wavelengths. The peak of the dispersion curve in the 2 μm–8 μm region is at 5 μm with a value of only -9.6 ps·nm^{-1}·km^{-1}. According to this small GVD, we pump 3-cm PCF with 100-fs pulses at 5 μm. At this pump wavelength, a peak power of 2.7 kW can generate an SC covering 2.7 μm–10 μm at a −30-dB level. The corresponding spectral evolution and the output SC are shown in Figs. 8(a) and 8(b), respectively. The spectrum broadening is also dominated by SPM and OWB. The spectrogram and the coherence of the obtained SC are depicted in Figs. 8(c) and 8(d), respectively, indicating the perfect coherence in the entire spectrum.

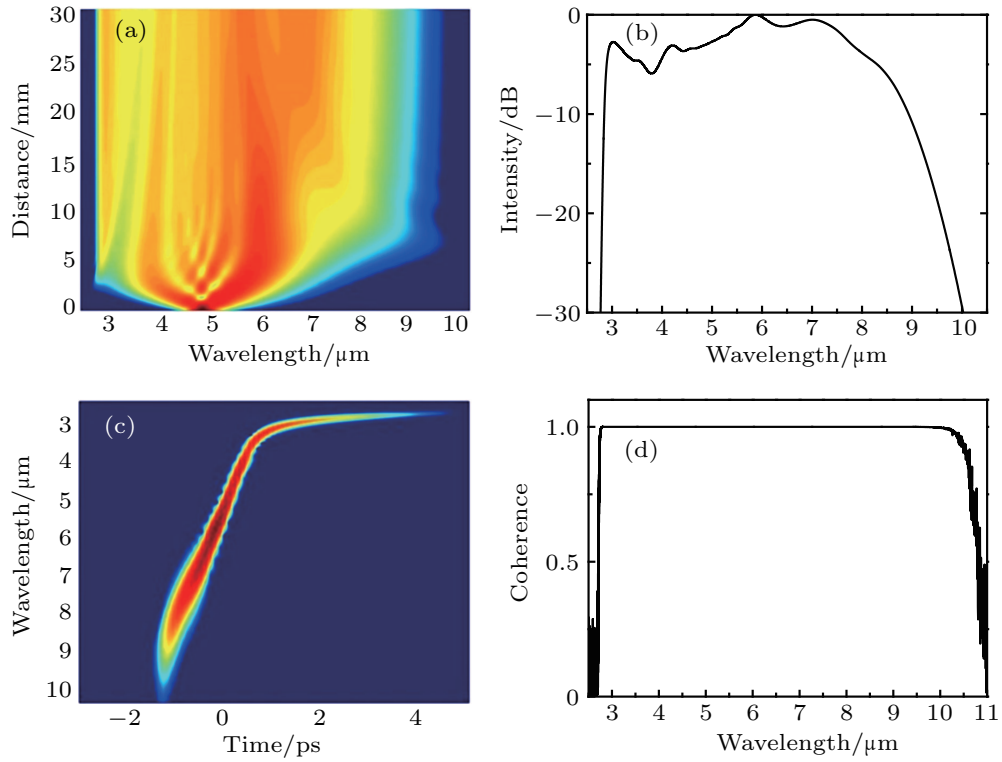


Fig. 8. (a) Simulated spectral evolution, (b) simulated spectral output, (c) simulated spectrogram, and (d) modulus of complex degree of first-order coherence of the output SC, with 3-cm chalcogenide PCF pumped at 5 μm with 100-fs pulses and 2.7-kW peak power.

5. Conclusions

In this paper, we proposed a novel As_2Se_3–As_2S_5 PCF. When $\Lambda = 3.2$ μm and $d = 1.6$ μm, the optimized near-zero flattened all-normal dispersion curve is obtained. Such dispersion characteristics provide a wide selection of pump wavelengths. The highly coherent SC covering 1.4 μm–10 μm is achieved when pumped at 3 μm. The generated SC covers 3-μm–5-μm and 8-μm–10-μm atmospheric windows. Furthermore, we investigate the influence of pulse parameters on the output SC. By using ultra-short pulses, the broadband and highly coherent SC spectrum can be generated. The simulation results provide a potential all-fiber realization of the broadband coherent MIR-SC.

References

[1] Amini-Nik S, Kraemer D, Cowan M L, Gunaratne K, Nadesan P, Alman B A and Miller R J D 2010 *Plos ONE* **5** e13053
[2] Salisbury J W and D'Aria D M 1994 *Remote Sens. Environ.* **47** 345
[3] Bekman H H P T, Heuvel J C, Putten F J M and Schleijpen H M A 2004 *Proc. SPIE* **5615** 27
[4] Steinmeyer G and Skibina J S 2014 *Nat. Photon.* **8** 814
[5] Zhao Z, Wu B, Wang X, Pan Z, Liu Z, Zhang P, Shen X, Nie Q, Dai S and Wang R 2017 *Laser Photon. Rev.* **11** 1700005
[6] Dudley J M, Genty G and Coen S 2006 *Rev. Mod. Phys.* **78** 1135
[7] Cimalla P, Walther J, Mittasch M and Koch E 2011 *J. Biomed. Opt.* **16** 116020
[8] Udem T, Holzwarth R and Hansch T W 2002 *Nature* **416** 233
[9] Al-Kadry A, Li L, Amraoui M E, North T, Messaddeq Y and Rochette M 2015 *Opt. Lett.* **40** 4687
[10] Liu L, Cheng T, Nagasaka K, Tong H, Qin Q, Susuki T and Ohishi Y 2016 *Opt. Lett.* **41** 392
[11] Nagasaka K, Liu L, Tuan T H, Cheng T, Matsumoto M, Tezuka H, Suzuki T and Ohishi Y 2017 *J. Opt.* **19** 095502

[12] Jiao K, Yao J, Zhao Z, Wang X, Si N, Wang X, Chen P, Xue Z, Tian Y, Zhang B, Zhang P, Dai S, Nie Q and Wang R 2019 *Opt. Express* **27** 2036
[13] Zhang N, Peng X, Wang Y, Dai S, Yuan Y, Su J, Li G, Zhang P, Yang P and Wang X 2019 *Opt. Express* **27** 10311
[14] Karim M R, Ahmad H and Rahman B M A 2017 *IEEE Photon. Technol. Lett.* **29** 1792
[15] Saini T S, Hoa N P T, Nagasaka K, Luo X, Tuan T H, Suzuki T and Ohishi Y 2018 *Appl. Opt.* **57** 1689
[16] Nagasaka K, Liu L, Tuan T H, Cheng T, Matsumoto M, Tezuka H, Suzuki T and Ohishi Y 2017 *Opt. Fiber Technol.* **36** 82
[17] Diouf M, Salem A B, Cherif R, Saghaei H and Wague A 2017 *Appl. Opt.* **56** 163
[18] Li Q, Liu L, Jia Z, Qin G, Ohishi Y and Qin W 2017 *J. Lightwave Technol.* **35** 4740
[19] Cherif R, Baili A and Zghal M 2013 *Proc. SPIE* **8772** 87720C
[20] Lagsgaard J 2007 *Opt. Express* **15** 16110
[21] Dudley J M and Taylor J R 2010 *Supercontinuum Generation in Optical Fibers* (Cambrige: Cambridge University)
[22] Frosz M H 2010 *Opt. Express* **18** 14778
[23] Cheng T, Usaki R, Duan Z, Gao W, Deng D, Liao M, Kanou Y, Matsumoto M, Misumi T, Suzuki T and Ohishi Y 2014 *Opt. Express* **22** 3740
[24] Klocek P 1991 *Handbook of Infrared Optical Materials* (New York: Marcel Dekker)
[25] Henderson-Sapir O, Jackson S D and Ottaway D J 2016 *Opt. Lett.* **41** 1676
[26] Salem A B, Cherif R and Zghal M 2011 *Opt. Express* **19** 19955
[27] Anderson D, Desaix M, Lisak M and Quiroga-Teixeiro M L 1992 *J. Opt. Soc. Am. B* **9** 1358